(16) Scanlan, J. J. Polym. Sci. 1960, 43, 501–508.
(17) Richardson, R. K.; Ross-Murphy, S. B. Int. J. Biol. Macromol. 1981, 3, 315–322.
(18) Clark, A. H.; Lee-Tuffnell, C. D. In Functional Properties of Food Macromolecules; Mitchell, J. R., Ledward, D. A., Eds.; Elsevier: Barking, U.K., 1986; pp 203–272.
(19) Lips, A.; Hart, P.; Clark, A. H. In Gums & Stabilizers for the Food Industry-4; Phillips, G. O., Wedlock, D. J., Williams, P. A., Eds.; IRL: Oxford, U.K., 1988, pp 39–50.
(20) Morris, E. R.; Rees, D. A.; Robinson, G. J. Mol. Biol. 1980, 138, 349–362.
(21) Clark, A. H. In Food Structure and Behavior; Blanshard, J. M. V., Lillford, P., Eds.; Academic: London, 1987; Vol. 1, pp 29–50.
(22) Gidley, M. J., third paper in a series in this issue.
(23) Oakenfull, D. G. J. Food Sci. 1984, 49, 1103–1110.

Molecular Mechanisms Underlying Amylose Aggregation and Gelation

Michael J. Gidley

Unilever Research Laboratory, Colworth House, Sharnbrook, Bedford, MK44 1LQ, U.K.
Received January 20, 1988; Revised Manuscript Received June 2, 1988

ABSTRACT: The molecular origin of the aqueous aggregation and gelation behavior of amylose is shown to lie in the formation of interchain double helices. Gelation is shown to be possible from "dilute" nonentangled amylose solutions, and no correlation is found between critical gelling concentrations and coil overlap concentrations for a range of amylose chain lengths. NMR and X-ray diffraction experiments show that amyloses precipitated from dilute aqueous solution contain only B-type aggregated double helices and that amylose gels contain rigid double-helical "junction zones" interconnected by more mobile amorphous single-chain segments. Optical rotation results suggest that the double-helix structure underlying amylose aggregation and gelation may have a left-handed conformation.

Introduction

In the previous two papers in this issue,[1,2] the aggregation and gelation behavior of enzymically synthesized and nearly monodisperse amylose samples has been described. These studies showed that polymer chain length has a profound effect on the aggregation processes that take place from (inherently unstable) aqueous amylose solutions. Thus the physical form (i.e., precipitate, gel, etc.), the kinetics of aggregation as monitored by turbidimetry[1,2] and rheology,[2] and the variation of gel strength with concentration[2] all show a dependence on the amylose chain length. The effects observed were rationalized on the basis of polymer–polymer cross-linking occurring over limited (typically less than 100 residues) regions of amylose chains.[1,2]

It is well established that amylose in aqueous solution has the hydrodynamic properties of a random coil.[3,4] Furthermore, it has been known for a long time that aged amylose gels show partial crystallinity[5] (as judged by X-ray diffraction). The diffraction pattern obtained from aqueous gels and precipitates is of the B type, characteristic of root, tuber, and stem granular starches.[6,7] It has recently been shown that B-type diffraction patterns are due to an ordered array of hexagonally packed double helices.[7] Although the helix packing arrangement in B-type crystallites appears to be well established, other structural details such as helix handedness[8] and packing sense[9] have still to be determined unambiguously.

From the above discussion, it can be seen that amylose aggregation/gelation eventually results in the conversion of at least some random coils into highly ordered crystalline structures. The molecular mechanisms involved in this conversion are the subject of current debate. Thus, Miles et al. have suggested[10] that gels are formed upon cooling molecularly entangled solutions as a result of phase separation, with subsequent crystallization occurring in the polymer-rich phase, whereas Sarko and Wu have proposed[11] that gelation occurs because of chain cross-linking by double-helical junction zones. The aim of our study was to examine the concentration regimes from which gelation occurs for amylose and to probe the molecular structures present and the transformations that occur during aqueous amylose aggregation.

Experimental Section

All amyloses were either synthesized enzymatically[1] or obtained commercially (potato amylose, Sigma), and solutions were prepared as described previously.[1,2]

Viscosity measurements were carried out at 303 K on a Contraves Low Shear 30 viscometer (Couette geometry—maximum shear rate 1 s^{-1}), extrapolated to "zero-shear" conditions,[12] and repeated 2–3 times for 2–3 replicates of the sample solution. For some aqueous amylose systems, viscosity values were found to increase markedly with time (1–5 min), suggesting the onset of polymer aggregation although visible signs of aggregation (e.g., turbidity, microgel formation) were not apparent. For characterization of the coil overlap concentration, aggregation effects need to be avoided, and therefore viscosity values were considered to be reliable only if essentially identical results were obtained following at least one repeat measurement on the same sample 1–2 min after the initial experiment.

X-ray diffraction measurements were made by using a Phillips powder diffractometer (PCW 1050/1390) mounted on a PW 1730/10 sealed tube X-ray generator operating at the Cu Kα wavelength (1.542 Å).

^{13}C NMR spectra were obtained on a Bruker CXP-300 instrument operating at 75.46 MHz, and spectra were referenced to external Me_4Si via the low-field resonance of solid adamantane (38.6 ppm). All ^{13}C spectra were obtained by using cylindrical sample holders in a double-bearing "solid" probe head (DB/MAS). For cross polarization and magic angle spinning spectra, spinning rates of 3–4 KHz and spin locking and ^1H decoupling fields of ~80 kHz (20 gauss) were employed. Other experimental parameters were as follows: acquisition time, 140 ms; recycle delay, 4 s; time domain points, 8 K, and transform size, 32 K. For ^1H NMR analysis, amylose samples were dissolved in D_2O (433 K, 15 min), lyophilized, and redissolved in D_2O. High-resolution ^1H NMR spectra were obtained on a Bruker AM200 instrument operating at 200.13 MHz. A 10-s delay between successive 90° pulses was employed to ensure complete relaxation. The variation of amylose signal area as a function of time and temperature was determined by comparison with the signal area due to a pyrazine standard in a coaxial tube. ^1H NMR T_2 values were determined by direct measurement of the free induction decay immediately following the initial 90° pulse in a Carr–Purcell–Meiboom–Gill (CPMG) pulse sequence as well as from the amplitudes of sub-

0024-9297/89/2222-0351$01.50/0

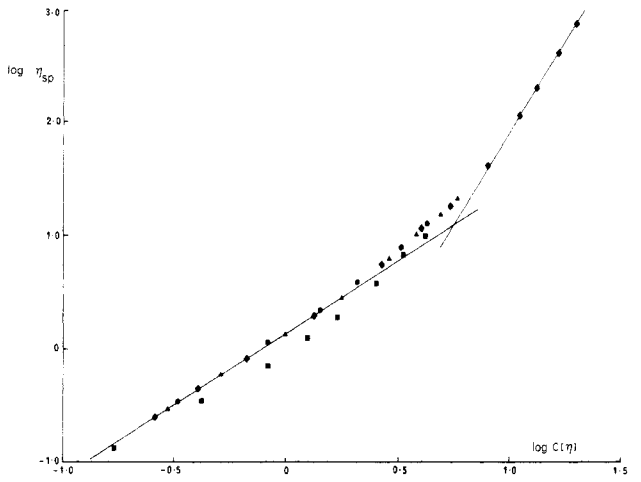

Figure 1. Variation of "zero-shear" specific viscosity (η_{sp}) with the coil overlap parameter ($C[\eta]$) for DP = 2800 (♦) and DP = 300 (▲) amyloses in dimethyl sulfoxide and DP = 2800 (●) and pea amylose (■, data from ref 10, Figure 3) in H_2O.

sequent spin echoes generated by the CPMG sequence, essentially as described by Ablett et al.[32]

Optical rotation was measured at 589 nm with a Perkin-Elmer 241MC polarimeter using a cell with either a 1-cm or, for turbid systems, a 0.1-cm path length. Temperatures were controlled by a programmable circulating water bath (Haake C/F3) in order to duplicate the time/temperature regimes used in high-resolution ^1H NMR and rheological[2] studies.

Results and Discussion

Concentration Regimes Leading to Precipitation and Gelation. Miles et al.[10] have proposed that amylose gelation takes place from molecularly entangled solutions whereas precipitation tends to occur below the so-called coil overlap concentration. These authors measured the variation of specific viscosity with concentration for aqueous solutions of a sample of pea amylose.[10] From a plot of log specific viscosity vs log concentration (Figure 3 in ref 10) a discontinuity was suggested to occur at ~1.45% (corresponding to concentration × intrinsic viscosity, $C[\eta] \sim 1.2$) at a specific viscosity of ~1. The gradients of the log specific viscosity vs log concentration plot below and above 1.45% were found to be ~1.0 and ~2.0, respectively.[10] These results were taken to show that coil overlap and molecular entanglements take place at >1.45%. However, the data of Miles et al.[10] show marked difference to the behavior reported for other polysaccharides.[12,13] For a wide range of random coil polysaccharides (e.g., dextran, alginate, λ carrageenan, carboxymethyl amylose,[12] and carboxymethyl cellulose[13]), as well as polystyrene in toluene,[12] discontinuity in log specific viscosity vs log concentration plots is observed at $C[\eta] \sim 4$, and specific viscosity ~ 10.[12,13] Gradients of such plots are found to be ~1.4 and ~3.3 below and above $C[\eta] \sim 4$, respectively.[12]

In an attempt to clarify the apparently anomalous behavior of aqueous amylose, we have investigated the variation of specific viscosity with concentration for enzymically synthesized amyloses. As aqueous solutions are difficult to study at high concentration due to aggregation, we have also investigated solutions of amylose in dimethyl sulfoxide; these solutions are stable at high (5–20%) concentration. Figure 1 shows the variation of zero-shear specific viscosity with concentration × intrinsic viscosity ($C[\eta]$) for solutions of DP = 2800 amylose in water (up to 5.0% w/v) and dimethyl sulfoxide (up to 15.0% w/v) and for dimethyl sulfoxide solutions of DP = 300 amylose (up to 20.0% w/v); the experimental data of Miles et al. (extracted from Figure 3 in ref 10) are also shown. Aqueous solutions of DP = 2550 amylose (up to 5.0% w/v) showed log η_{sp} vs log $C[\eta]$ behavior essentially identical with that of DP = 2800. Amyloses of shorter chain length could only be studied at concentrations corresponding to $C[\eta] < 1.4$ due to lower intrinsic viscosities and more rapid aggregation[1] but, in this range, showed log η_{sp} vs log $C[\eta]$ behavior identical with that shown in Figure 1.

The data obtained in this study agree well with previous results for random coil polysaccharides.[12,13] Thus, if straight lines are constructed for high and low concentrations (Figure 1), gradients of 1.28 and 3.35, respectively, are found, and an intersection (discontinuity) occurs at $C[\eta] \sim 5.5$ and $\eta_{sp} \sim 12$. The analysis of log η_{sp} vs log $C[\eta]$ data by two straight lines is almost certainly an oversimplification, particularly in the region of the "discontinuity". The present data show that specific viscosities for concentrations in the range $1.8 < C[\eta] < 7.5$ are higher than predicted on the basis of a sharp discontinuity. Similar behavior is apparent[14] for other polysaccharides[12] and is particularly pronounced for (hydroxyethyl)cellulose[13] and xanthan.[15] It has been proposed[13-15] that two discontinuities are present in the log η_{sp} vs log $C[\eta]$ behavior of polysaccharides; indeed, our present data could be represented in this way by an additional line from $C[\eta] \sim 1.8$, $\eta_{sp} \sim 2.8$, to $C[\eta] \sim 8$, $\eta_{sp} \sim 40$. An alternative explanation, which we favor, is that there is a gradual transition from dilute solution behavior (isolated coils) through increasing degrees of coil overlap to a molecularly entangled semidilute solution. Discontinuities (critical concentrations) in the concentration dependence of experimentally determined properties (e.g., light scattering, solution and melt viscosities) are known to occur over a range of $C[\eta]$ values reflecting the gradual nature of coil interpenetration with increasing concentration.[16]

The data of Miles et al.[10] show somewhat lower specific viscosities at equivalent $C[\eta]$ values compared to our data (Figure 1), possibly due to the polydisperse nature of the pea amylose fraction or to shear thinning in the Ubbelohde capillary viscometer used in their study. A further complication in the study by Miles et al.[10] could be the test employed to demonstrate the absence of aggregation, i.e., solution clarity. We have found that significant aggregation occurs for synthetic amyloses with a DP (2550, 2800) similar to that of the pea amylose fraction ($DP_w \sim 3000$) used by Miles et al.[10] without loss of visually assessed optical clarity (see Experimental Section).

The present data suggest that aqueous amylose solutions do not deviate from dilute solution behavior (i.e., are not significantly entangled) below $C[\eta] \sim 1.8$. If phase separation arising from molecular entanglement is important in amylose gelation, this concentration would be expected to be similar to the critical gelling concentration. For amylose of DP = 2800, intrinsic viscosity in water is calculated[4] to be 0.76 dL g^{-1}; $C[\eta] \sim 1.8$ therefore corresponds to a concentration of 2.3–2.4%. This value is more than double the observed[1] critical gelling concentration of 1.0 ± 0.2%. For amyloses of DP = 1100, 660, and 300, $C[\eta] \sim 1.8$ corresponds to concentrations of 3.8%, 4.9% and 7.2%, respectively, compared to observed critical gelling concentrations[1,2] of 0.8–1.1%, showing that critical gelling concentration does not scale with coil overlap concentration. It is therefore clear that, for nearly monodisperse amyloses, molecular entanglement does not determine the critical gelling concentration, as gelation is observed at concentrations significantly lower than those leading to nondilute solution behavior (Figure 1). A similar nonequivalence of critical gelling concentration and coil overlap

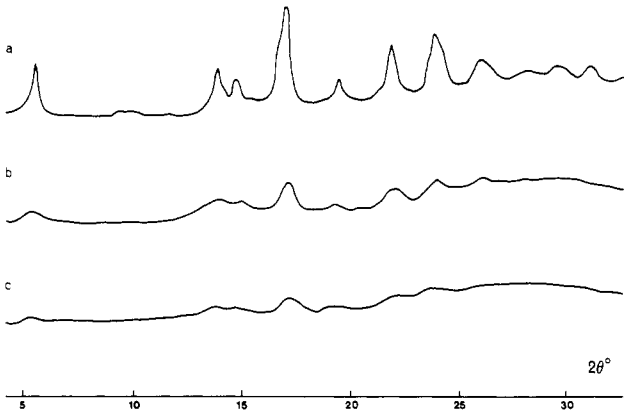

Figure 2. X-ray diffraction patterns of amyloses precipitated from 0.8% aqueous solution for monodisperse samples of DP = (a) 40, (b) 110, and (c) 250.

concentration has been noted for globular proteins by Clark and Ross-Murphy,[17,18] who also pointed out that gelation would be expected to occur at suboverlap concentrations if cross-links have finite energy.[17] This latter condition is apparently true for amylose gels formed at ambient temperature, as melting occurs in the temperature range 140–160 °C.[1,19]

Characterization of Ordered Molecular Structures in Amylose Aggregates and Gels. The results discussed in the preceding section show that gelation of monodisperse amyloses can take place from dilute (i.e., nonentangled) aqueous solutions. This suggests that a specific cross-linking mechanism is operative. For gelling polysaccharides,[20] specific cross-linking involves the cooperative interaction of many residues from each participating chain such that the enthalpy gained from the sum of noncovalent interchain interactions is sufficient to outweigh the entropic loss suffered by chains involved in cross-linking.[20] Such regions of interchain binding are called junction zones and consist of conformationally ordered chain segments.[20] It is well-known that aged amylose gels are partially crystalline,[5,10] i.e., contain ordered arrays of double helices.[7]

In order to examine the hypothesis that amylose gels contain junction zones formed from interchain double helices, probes of ordered molecular structure are required. X-ray diffraction is sensitive to long-range ordering of double helices (i.e., crystalline domains) but would not be expected to detect isolated double helices or small aggregates. We have recently shown that cross polarization and magic angle spinning (CP/MAS) ^{13}C NMR spectroscopy provides information on solid starch samples which complements that available from X-ray diffraction.[21] NMR spectroscopy is sensitive to structural effects at the molecular level and therefore would be expected to detect individual double helices whether or not they are present in extended ordered arrays. By use of ^{13}C CP/MAS NMR it was shown that native granular starches contain a mixture of double helices and amorphous α-(1→4) glucan.[21]

Figures 2 and 3 show X-ray diffraction patterns and ^{13}C CP/MAS NMR spectra, respectively, of amyloses of DP = 40, 110, and 250 precipitated from 0.8% aqueous solution. Diffraction patterns recorded before and after NMR spectroscopy were identical. Precipitated DP40 amylose has (Figure 2a) a well-resolved B-type X-ray diffraction pattern (similar to that obtained from lower molecular weight material[22]), suggesting that much of the amylose is present in ordered double-helical arrays. X-ray diffraction patterns for precipitated amyloses of DP = 110 and 250 (Figure 2b,c) show much broader and less intense diffraction peaks, suggesting that crystallization into ordered arrays is less extensive and/or crystalline domains

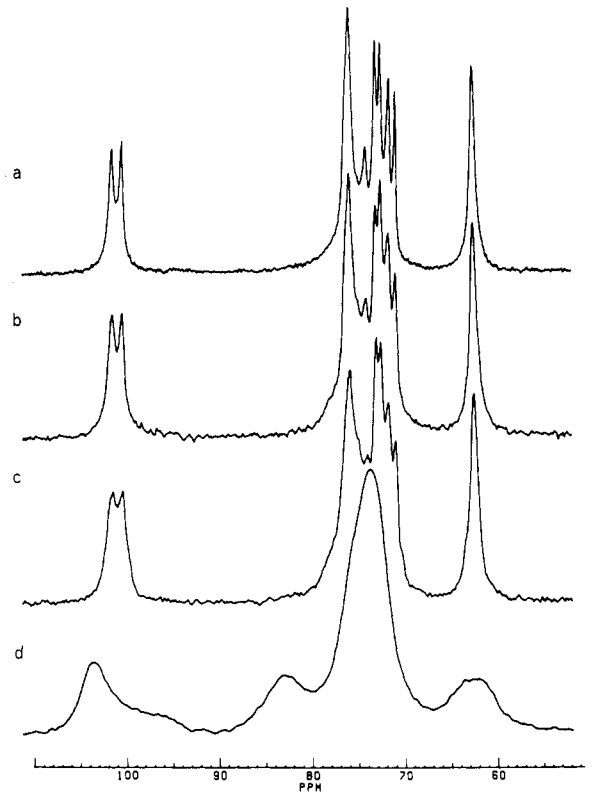

Figure 3. ^{13}C CP/MAS NMR spectra of amyloses precipitated from dilute aqueous solution having chain lengths (DP) of (a) 40, (b) 110, and (c) 250 and (d) amorphous α-(1→4) glucan.[21] Spectra a–c were obtained on the samples used for X-ray diffraction analysis (Figure 2a–c, respectively).

are smaller than for precipitated DP = 40 amylose (Figure 2a).

The ^{13}C CP/MAS spectrum of precipitated DP = 40 amylose (Figure 3a) shows narrow signals characteristic of a highly ordered solid. The doublet observed for C-1 sites of B-type material (~100 ppm) reflects the fact that there are two glucose residues in the asymmetric unit[7,23] and has been rationalized[21] in terms of the symmetry of helix packing. Signals in the 70–75 ppm region are assigned to C-2,3,4,5 sites and show more than one resonance for each carbon site. On the basis of the relative intensities observed, two resolved doublets (70.3 and 71.0 ppm, 71.9 and 72.5 ppm), one overlapping doublet (73.5 and ~75.4 ppm), and a single peak/unresolved doublet (75.4 ppm) may be proposed for this spectral region. These observations are in line with the expectation that C-2,3,4,5 sites should have the same multiplicity as C-1 sites if such multiplicities reflect the number of glucose residues in the asymmetric unit. Figure 3a shows increased resolution compared to most previously reported spectra of B-type materials.[21,23-25] This may be due to the use of nearly monodisperse amylose[26] and/or the double-bearing sample rotor employed, which, in our experience, leads to narrower resonances for crystalline material than a conventional Andrews "bullet" rotor.

Figure 3d shows the spectrum of amorphous α-(1→4) glucan.[21] Apart from broader signals, marked chemical shift differences in comparison with B-type amylose spectra are apparent[21] (Figure 3). Thus signal intensity at ~103 and 80–83 ppm is characteristic of amorphous α-(1→4) glucan. Comparison of Figure 3d with Figures 3a–c shows that precipitated amylose has no detectable (<5%) amorphous component. The major difference between parts a–c of Figure 3 is the spectral resolution, which becomes markedly less with increasing chain length. As

there is no amorphous component in these spectra, essentially all material must be in an ordered (double-helical) form. If, as has been proposed,[21] multiplet splitting is due to interhelix interactions, then a decrease in resolution is explicable in terms of less perfect helix packing. The differences observed in X-ray diffraction patterns (Figure 2) are consistent with this explanation. ^{13}C CP/MAS NMR spectroscopy therefore suggests that amylose precipitated from dilute aqueous solution is essentially completely ordered (helical) on a molecular level but has increasing perfection of helix packing with decreasing chain length for DP = 250, 110, and 40. These results are consistent with the deductions[1] that, when aggregated, DP = 40 amylose is not cross-linked, DP = 110 amylose is lightly cross-linked, and DP = 250 amylose is extensively cross-linked,[1] as cross-linking would be expected to impede the growth of "crystalline" arrays of double helices.

Having established the molecular structures present in amyloses precipitated from dilute aqueous solutions, we now examine whether similar structures are present in aqueous amylose gels. Previous X-ray diffraction experiments[5,10] have shown the presence of B-type crystallization in amylose gels. We have examined aqueous 10% w/v gels of three amylose samples, synthetic monodisperse amyloses of DP = 300 and 2800, and a polydisperse potato amylose of $DP_w \sim 3000$ by X-ray diffraction. All gels showed very weak B-type diffraction patterns with peak widths similar to those in Figure 2c but with much reduced intensities. Gels of DP = 300 amylose showed the most intense patterns ($\sim$5% of the intensity of Figure 2c) suggesting substantial crystallization, whereas gels of the two amyloses of higher molecular weight showed much weaker patterns (<1% of the intensity of Figure 2c). Similarly, as found for gels of lower concentration,[1,2] turbidity was much greater in 10% gels of DP = 300 amylose compared to 10% gels of the other two amyloses. This is probably due, at least in part, to precipitation within the gel[1,2] which would be expected (Figure 2) to result in crystalline B-type structures. Gels of higher molecular weight amylose show no evidence for precipitation and have weaker X-ray diffraction patterns. In all cases, gels were examined after storage at 293 K for 2 h, 2 days, and 8 days, and diffraction patterns were found to be essentially identical for each of the gels following the various storage times.

The gels characterized by X-ray diffraction were also examined by NMR spectroscopy. Figure 4a shows the single-pulse excitation ^{13}C NMR spectrum (i.e., conventional high-resolution experiment) on a 10% amylose gel. Broad spectral features are apparent in the expected[27] chemical shift ranges for α-(1→4) glucans. There are at least three reasons why such broad resonances may be observed, namely, a decrease in ^{13}C T_2 values, a dispersion of chemical shifts, or chemical shift anisotropy induced by network formation. If the latter mechanism is operative, then magic angle spinning (which effectively removes chemical shift anisotropy[28]) would be expected to lead to narrower resonances. Conversely, if either T_2 or chemical shift dispersion effects are responsible, then magic angle spinning should have little effect. The observation (Figure 4b) of narrower resonances following magic angle spinning at 500 Hz (i.e., comparable to the frequency width of the broadest resonance in Figure 4a) therefore supports the idea that chemical shift anisotropy is responsible for the width of resonances in Figure 4a. Amylose gels thus contain some polysaccharide, which has sufficient segmental motion for chemical shifts to be averaged on the NMR time scale but which experiences chemical shift anisotropy due to the network-based structure. The

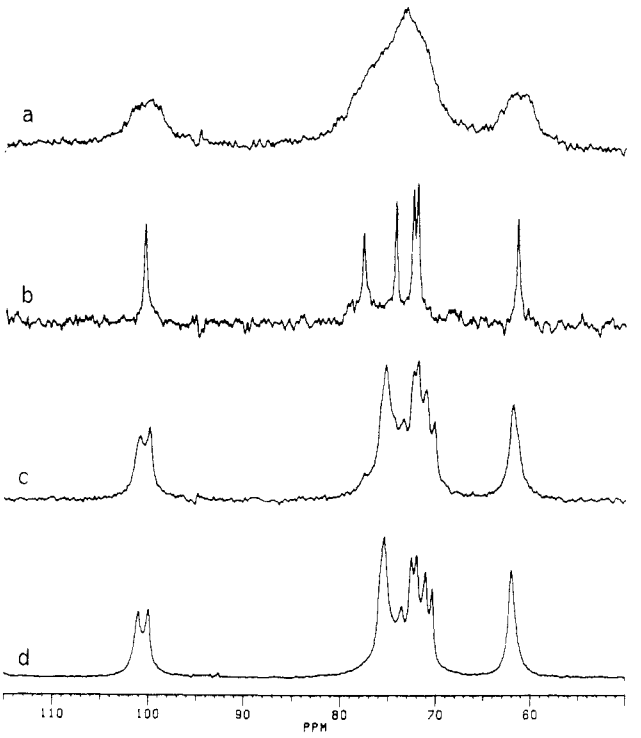

Figure 4. (a) ^{13}C single-pulse spectrum of a 10% w/v gel of DP = 2800 amylose obtained by using high-power ^1H decoupling; (b) spectrum a with magic angle spinning at 500 Hz; (c) ^{13}C CP/MAS spectrum of the same amylose gel; (d) ^{13}C CP/MAS spectrum of solid B-type amylose (as in Figure 3a).

chemical shifts of resonances in Figure 4b (100.5, 77.7, 74.4, 72.5, 72.1, and 61.5 ppm) are identical (±0.1 ppm) with those found for aqueous solution of amylose and other α-(1→4) glucans, obtained under the same experimental conditions. This suggests that the conformations adopted by the mobile amylose segments within the gel are very similar to those found in solution.

The more immobile "solidlike" regions in a polysaccharide gel should be amenable to study by ^{13}C CP/MAS NMR[29] provided that care is taken to check that the high spinning speeds employed do not significantly affect the gel under study. In our experience, amylose gels of <5% w/v concentration are unstable under fast (3-kHz) spinning conditions and are broken up with significant loss of water. However, 10% w/v amylose gels are found to be affected minimally by the experimental conditions as judged by visual observation, the fact that multiple repeats of the CP/MAS experiment on the same gel lead to the same quantitative results (see below), and the observations of identical X-ray diffraction patterns before and after CP/MAS analysis. The ^{13}C CP/MAS spectrum of a 10% w/v amylose gel is shown in Figure 4c and is found to be essentially identical with that obtained from crystalline B-type solid material (Figures 3 and 4d), thereby showing that the solidlike polysaccharide in the gel is present as aggregated double helices.

The results shown in Figure 4 are exactly those which might be expected if amylose gels contain double-helical junction zones connected by more mobile single-chain segments. In order to determine whether the two conformational states characterized by their differing mobilities (Figure 4a,c) are the only ones present, a ^{13}C CP/MAS spectrum was obtained for a frozen gel at 233 K. At this temperature, all of the polysaccharide in the sample would be sufficiently solidlike to be detected by a CP/MAS experiment. The spectrum thus obtained (Figure 5b) is found to be simulated accurately (Figure 5a)

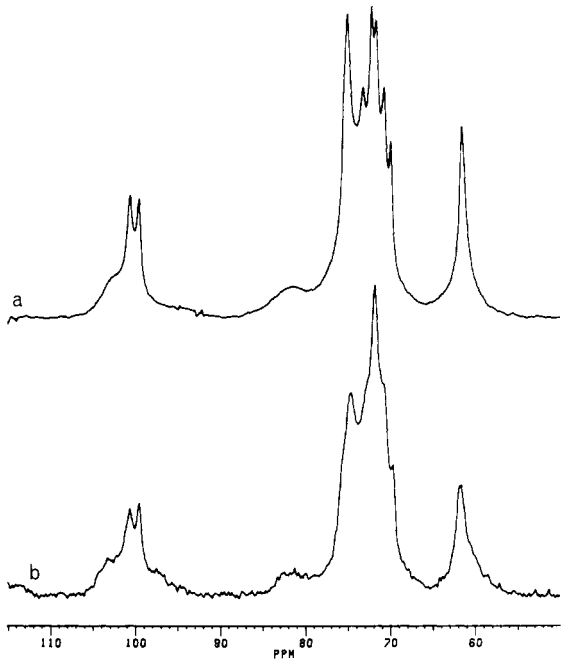

Figure 5. (a) Simulated ^{13}C CP/MAS spectrum obtained by adding 67% of the spectral intensity of Figure 3a (B-type solid) with 33% of the intensity of Figure 3d (amorphous solid); (b) ^{13}C CP/MAS spectrum of a 10% DP = 2800 amylose gel at 233 K.

by a combination of spectra due to B-type double-helical amylose (Figure 3a) and amorphous material (Figure 3d). The ^{13}C CP/MAS spectra of frozen aqueous α-(1→4) glucan solutions[30] are found to be essentially identical with those of amorphous solid material, suggesting that α-(1→4) glucan solutions contain the same range of conformations as amorphous solids.[30] These experiments therefore provide evidence that the two conformational states corresponding to "rigid" and "mobile" amylose segments are due to double helix and amorphous solutionlike conformations, respectively, and account for all of the amylose in 10% aqueous gels.

The quantitative simulation of frozen gel CP/MAS spectra (Figure 5) allows an estimate of the proportions of the two conformational states to be made.[31] In this way, the double helix content in 10% amylose gels was estimated to be 67%, 67%, and 83% (±2%) for potato, DP = 2800, and DP = 300 amyloses, respectively. The markedly higher double helix content in the DP = 300 gel is consistent with the observed relative X-ray diffraction identities (vide infra).

As a further quantitative probe of polysaccharide mobility, we also investigated the ^1H T_2 values of amylose gels in D_2O by directly measuring the decay of total magnetization following a Carr–Purcell–Meiboom–Gill pulse sequence.[32,33] The magnetization decay of amylose protons could in all cases be modeled accurately by assuming two ranges of relaxation behavior corresponding to T_2 values of ~10 μs and 1–10 ms, respectively. A previous investigation of a 3% w/v amylose gel showed a similar distinction of two relaxation time scales having T_2 values of ~40 μs and 3–30 ms.[34] The relative proportion of the total decay attributable to the two relaxation time scales could be calculated from observed magnitudes. The proportion of protons exhibiting ~10-μs T_2 values was found to be 70%, 72%, and 88% (±2%) for 10% w/v potato, DP = 2800, and DP = 300 amylose gels, respectively. These values may be compared with analyses of ^{13}C CP/MAS spectra of frozen H_2O gels (Figure 5), which gave estimates of double helix content of 67%, 67%, and 83%, respectively, for the same three amylose samples. For each of the three gels, quantitative values obtained from both ^1H magnetization decays and low-temperature (233 K) ^{13}C CP/MAS spectra were identical following storage for 2 h, 2 days, or 8 days at 293 K. The reasonable quantitative agreement between ambient ^1H T_2 measurements and low-temperature ^{13}C CP/MAS spectral simulation provides further evidence for the existence of two conformational states having widely different mobilities. Amylose gels are therefore suggested to contain rigid, double-helical segments (^1H T_2 ~ 10 μs for 10% gels) which act as junction zones and more mobile, amorphous interjunction segments (^1H T_2 = 1–10 ms for 10% gels).

On the Structure of B-Type Amylose. The detailed molecular structure of B-type double-helical amylose is the subject of current debate. The pioneering X-ray fiber diffraction study of Wu and Sarko[7] suggested that the structure is based on parallel-stranded double helices packed in an hexagonal array with individual strands in a sixfold helical conformation with a rise per residue (H) of ~0.35 nm. Further structural details were proposed on the basis of X-ray refinement procedures,[7] e.g., that individual strands have right-handed conformations and that helices are packed in an antiparallel fashion.[7] These latter two structural features have recently been questioned.[8,9] The postulation of antiparallel packing would be difficult to reconcile[9] with current models of starch biosynthesis[6] in which adjacent branches of amylopectin molecules are thought to form double-helical arrays[6] of either A or B type, depending on the branch length.[35,36] The proposed right-handed structure for B-type amylose[7] has been questioned on the basis of optical rotation results.[8] Rees[37] has developed a quantitative link between optical rotation and glycosidic torsion angles ϕ and Ψ[38] which has successfully[20,38] accounted for the optical rotation of many oligosaccharides, as well as the coil and double helix conformations of agarose and ι-carrageenan.[8] Wu and Sarko[7] showed that the possible conformations for B-type amylose helices that could fit the unit-cell dimensions were limited to two small ranges of angles ϕ and Ψ corresponding to one left-handed and one right-handed structure. From a comparison of calculated[38] optical rotation values at 589 nm for such right-handed (74°) and left-handed (190°) double helices (using the conformations suggested by Wu and Sarko[7]), with the observed optical rotation of amylose solutions and gels (195°), Rees[8] proposed that B-type amylose may be left-handed instead of the proposed[7] right-handed structure. Furthermore, the related A-type amylose polymorph has recently been suggested to be composed of left-handed double helices[39] rather than the right-handed double helices proposed for A-type amylose by Wu and Sarko.[40]

We have reinvestigated the optical rotation of amylose solutions and gels using a number of monodisperse amyloses covering a range of chain lengths. As described previously,[1,2] hot aqueous solutions of each of these materials (DP = 40–2800) develop turbidity on cooling with amyloses of DP < 110 forming precipitates and longer chain amyloses (DP > 250) forming gels at >1.0% concentration.[1] Optical rotation measurements cannot be obtained from highly turbid samples such as extensively aggregated amyloses; there is, therefore, a point during the progressive aggregation of amylose systems after which no further optical rotation readings can be taken due to sample turbidity. For some gelling amyloses, a further problem was encountered; namely, at some stage following gelation, large fluctuations in readings were noted. These fluctuating readings were found to be markedly different on reversing the polarimeter cell and were sensitive to

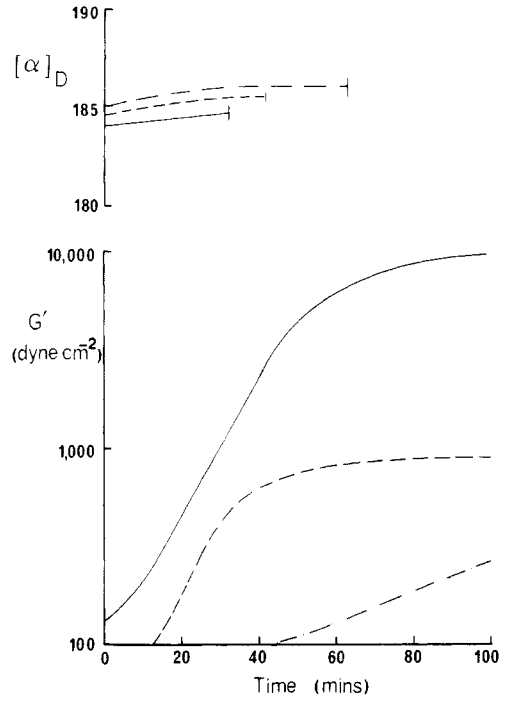

Figure 6. Time course of G' evolution (lower traces, taken from ref 2, Figure 3) and optical rotation (upper traces) for 2% amyloses of DP = 2500 (-·-), 110 (—), and 400 (---) upon cooling from 333 to 298 K at 1 K min^{-1} and holding at 298 K. Bars terminating optical rotation traces represent the time after which no further readings could be taken due to turbidity and/or birefringence/scattering effects.

application of slight pressure onto the amylose gel. It seems likely that these observations are due to birefringence or light-scattering effects induced by annealing processes in the cross-linked network structure. Despite the two limitations described above, optical rotation measurements could be obtained on a number of systems which showed evidence of aggregation and network formation.

A number of optical rotation experiments were carried out on 2% aqueous amyloses, following the time/temperature course used for G' measurements (ref 2, Figure 3). In all cases, molar optical rotation at 589 nm was found to be unchanged (185° ± 2°) following the onset of gel formation until turbidity/birefringence effects precluded further measurements. Representative data are presented in Figure 6 from which it can be seen that significant modulus development occurs without any change in optical rotation for a range of amylose chain lengths. The DP = 400 and 1100 systems also showed significant turbidity (cf. ref 2, Figure 5) with no detectable change in optical rotation.

It could be argued that the lack of change in optical rotation (Figure 6) reflects the involvement of only a small percentage of amylose residues in an ordered (double-helical) conformation. In order to quantify the adoption of ordered conformations in aggregating amylose systems, we have monitored the ^{1}H NMR signal area of DP = 400 amylose solutions during cooling-induced aggregation. High-resolution NMR line widths of ordered polysaccharides are usually too large to be resolved from the spectral base line,[20,41] and therefore residual NMR signal intensity provides an index of the extent of conformational ordering.[20,41] Figure 7 shows optical rotation and ^{1}H NMR signal area data for 1% and 3% DP = 400 amylose in D_2O during the same controlled cooling regimes (optical rotation behavior was found to be essentially identical for amylose in D_2O and H_2O). Molar optical rotation at 589

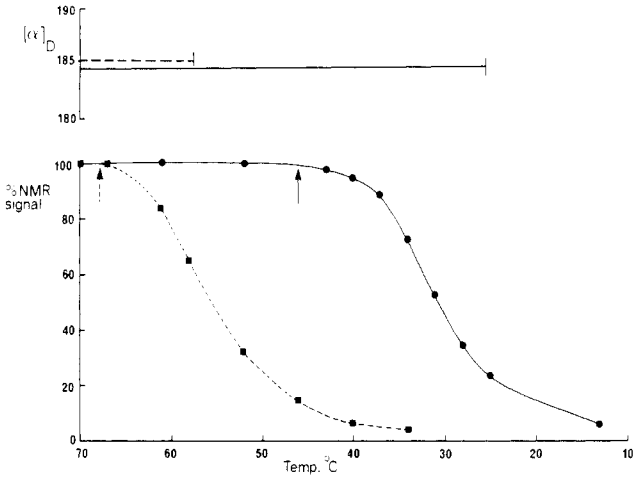

Figure 7. Comparison of high-resolution ^{1}H NMR signal area relative to coaxial pyrazine (lower traces) and optical rotation (upper traces) as a function of temperature for 1% (—) and 3% (---) DP = 400 amylose in D_2O cooled from 343 at 0.15 K min^{-1}. Arrows indicate the temperature at which turbidity first became apparent. Bars terminating optical rotation traces correspond to the temperature below which turbidity/birefringence effects precluded further measurements.

nm was found to be 185° ± 2° for both 1% and 3% DP = 400 amylose systems following loss of ~70% and ~40% of the ^{1}H NMR signal area, respectively (Figure 7). This suggests that the true optical rotation of the ordered double-helical structure is very similar to the value observed. The observed temperatures of turbidity onset are found to be similar to the onset of NMR signal loss (Figure 7) and suggest that turbidity development is linked to adoption of the ordered structure.

The data presented in Figures 6 and 7 therefore show that the molar optical rotation at 589 nm is 185° ± 2° for both aqueous amylose solutions and partially aggregated amyloses; the data suggest that the true optical rotation of the ordered structure is also ~185°. This result is consistent with the observation[42] of similar vacuum ultraviolet circular dichroism spectra for amylose solutions and gels,[42] as the electronic transitions observed directly by circular dichroism also determine the optical rotation behavior at longer wavelengths.[20] We have shown earlier that 10% aqueous amylose gels contain ordered arrays of B-type double helices. Miles et al.[10] have shown that B-type crystallinity is also present in less concentrated amylose gels (2.4–7.0%), and we have confirmed these findings with 2.0% and 3.0% w/v DP = 400 amylose gels aged for 24 h. However, we have not been able to detect unambiguously the presence of double-helical structures (by ^{13}C CP/MAS NMR or X-ray diffraction) at the same time as obtaining reliable optical rotation results. Nevertheless, on the evidence of the present study, the most likely molecular basis for amylose aggregation appears to be the adoption of double-helical structures (which causes loss of high-resolution ^{1}H NMR signals and can be directly detected in solids and concentrated gels by ^{13}C CP/MAS NMR) followed by helix–helix aggregation thereby leading to turbidity effects and, for sufficiently long amylose chains,[1,2] cross-linked network formation and gelation. If this model is correct, then the ordered structure adopted initially is the same as that found following extensive helix–helix aggregation, i.e., the B-type structure.

Our results therefore support the suggestion made by Rees[8] that individual strands in the B-type double helix adopt a left-handed conformation. Definitive determination of the handedness of the amylose B-type double helix will probably require X-ray diffraction analysis of more

highly crystalline samples than have previously been studied, e.g., crystallized amylose oligomers.[22,43] It is interesting to note, however, that the crystal structure of methyl-α-maltotrioside,[44] the highest oligomer yet studied by direct X-ray methods, involves a left-handed conformation with a similar rise per residue (0.36 nm[44]) as that found for double-helical amylose (0.35 nm[7]) and torsion angles ($\phi = -38°$, $\Psi = 30°$)[42] similar to those which would be required for left-handed double helices to fit into the B-type unit cell.[7] The predicted[38] optical rotation for a polymer helix based on the trimer crystal structure[44] is 206°, which is sufficiently close to our observed values in gels of ~185° to suggest that the double-helical conformation may be similar to that of the trimer.[44]

The most likely explanation for the observation of essentially identical optical rotation values for amylose solutions and double helices is that the weighted average of all the conformations adopted in solution is very similar to the fixed double-helical conformation. Some support for this suggestion can be obtained from NMR data. Thus, we have shown recently[45] that the C-1 chemical shift in ^{13}C CP/MAS spectra of solid α-(1→4) glucans is primarily determined by the glycosidic conformation.[45] The observation of essentially identical C-1 chemical shifts for amylose solutions (100.5 ppm, cf. Figure 4b) and the average shift for the C-1 doublet of solid B-type amylose (100.45 ppm, Figure 4c,d) is therefore consistent with the fixed double-helical conformation being similar to the weighted average of solution conformations. The similarity of C-1 solid-state shifts for A- and B-type α-(1→4) glucans also suggests that these two polymorphs involve similar double-helical conformations, as suggested by Wu and Sarko.[11] Recent structural studies of A-type amylose have also led to the proposal[39] of a left-handed double-helical structure.

Conclusions

Based on our studies of the properties of essentially monodisperse amyloses covering a range of chain lengths, the following conclusions may be drawn concerning the molecular mechanisms involved in amylose aggregation and gelation.

The critical concentration for gelation is nearly independent of chain length (~1.0% w/v) and is always significantly lower than the concentration at which rheological consequences of molecular entanglement are observed (2.3–7.2% w/v depending on the chain length), therefore suggesting that a specific molecular interaction underpins amylose gelation.

The only detectable (by ^{13}C CP/MAS NMR) molecular structure present in precipitates deposited from dilute aqueous amylose solutions is the B-type double helix. X-ray diffraction and ^{13}C CP/MAS NMR show that the perfection of crystalline packing in these precipitates is inversely related to the amylose chain length.

Concentrated (10% w/v) amylose gels contain two distinct molecular structures: rigid B-type double helices and more mobile amorphous single chains. The relative abundance of these two conformations may be obtained either from low-temperature ^{13}C CP/MAS NMR spectra or from analysis of ^{1}H T_2 values at ambient temperature. A model for amylose gelation involving double-helical junction zones connected by amorphous "elastically active" single chains is proposed.

Optical rotation studies suggest that individual strands in the B-type (and A-type) double-helical structures may adopt a left-handed conformation rather than the right-handed structure proposed on the basis of X-ray fiber diffraction analysis.

In summary, it is proposed that amylose aggregation and gelation phenomena are dominated by the formation and subsequent aggregation of B-type double helices and that individual strands in these helices may have a left-handed structure.

Note Added in Proof. New three-dimensional structures of A- and B-type amylose have recently been reported[46,47] with both structures based on similar left-handed double helices. The predicted[37] optical rotation at 589 nm of the new B-type structure[47] is ~195°, in good agreement with the results reported above.

Acknowledgment. I thank S. Bociek, S. Ablett, and D. Caswell for obtaining NMR data and H. McEvoy and S. B. Ross-Murphy for advice concerning rheological measurements.

Registry No. Amylose, 9005-82-7.

References and Notes

(1) Gidley, M. J.; Bulpin, P. V., first paper in a series in this issue.
(2) Clark, A. H.; Gidley, M. J.; Richardson, R. K.; Ross-Murphy, S. B., second paper in a series in this issue.
(3) Banks, W.; Greenwood, C. T. *Starch and its Components*; Edinburgh University: Edinburgh, 1975.
(4) Ring, S. G.; L'Anson, K. J.; Morris, V. J. *Macromolecules* **1985**, *18*, 182–188.
(5) Katz, J. R. *Z. Phys. Chem., Abt. A* **1930**, *150*, 37–59.
(6) French, D. *Starch: Chemistry and Technology*, 2nd ed; Academic: New York, 1984; pp 184–247.
(7) Wu, H.-C. H.; Sarko, A. *Carbohydr. Res.* **1978**, *61*, 7–25.
(8) Rees, D. A. *Pure Appl. Chem.* **1981**, *53*, 1–14.
(9) Wild, D. L.; Blanshard, J. M. V. *Carbohydr. Polym.* **1986**, *6*, 121–143.
(10) Miles, M. J.; Morris, V. J.; Ring, S. G. *Carbohydr. Res.* **1985**, *135*, 257–269.
(11) Sarko, A.; Wu, H.-C. H. *Stärke* **1978**, *30*, 73–78.
(12) Morris, E. R.; Cutler, A. N.; Ross-Murphy, S. B.; Rees, D. A.; Price, J. *Carbohydr. Polym.* **1981**, *1*, 5–21.
(13) Castelain, C.; Doublier, J. L.; Lefebvre, J. *Carbohydr. Polym.* **1987**, *7*, 1–16.
(14) Launay, B.; Doublier, J. L.; Cuvelier, G. *Functional Properties of Food Macromolecules*; Elsevier: London, 1986; pp 1–78.
(15) Cuvelier, F.; Launay, B. *Carbohydr. Polym.* **1986**, *6*, 321–333.
(16) Aharoni, S. M. *J. Macromol. Sci., Phys.* **1978**, *B15*, 347–370.
(17) Clark, A. H.; Ross-Murphy, S. B. *Adv. Polym. Sci.* **1987**, *83*, 57–192.
(18) Clark, A. H.; Ross-Murphy, S. B. *Br. Polym. J.* **1985**, *17*, 164–168.
(19) Eberstein, K.; Höpcke, R.; Konieczny-Janda, G.; Stute, R. *Stärke* **1980**, *32*, 397–404.
(20) Rees, D. A.; Morris, E. R.; Thom, D.; Madden, J. K. *The Polysaccharides*; Academic: New York, 1982; Vol. 1, pp 195–290.
(21) Gidley, M. J.; Bociek, S. M. *J. Am. Chem. Soc.* **1985**, *107*, 7040–7044.
(22) Gidley, M. J.; Bulpin, P. V. *Carbohydr. Res.* **1987**, *161*, 291–300.
(23) Veregin, R. P.; Fyfe, C. A.; Marchessault, R. H.; Taylor, M. G. *Macromolecules* **1986**, *19*, 1030–1034.
(24) Horii, F.; Hirai, A.; Kitamaru, R. *Macromolecules* **1986**, *19*, 930–932.
(25) Hewitt, J. M.; Linder, M.; Perez, S.; Buleon, A. *Carbohydr. Res.* **1986**, *154*, 1–13.
(26) Horii, F.; Yamamoto, H.; Hirai, A.; Kitamaru, R. *Carbohydr. Res.* **1987**, *160*, 29–40.
(27) Gidley, M. J. *Carbohydr. Res.* **1985**, *139*, 85–93.
(28) Yannoni, C. S. *Acc. Chem. Res.* **1982**, *15*, 201–208.
(29) Stipanovic, A.; Giammatteo, P. J.; Robie, S. B. *Biopolymers* **1985**, *24*, 2333–2343.
(30) Gidley, M. J.; Bociek, S. M. *Carbohydr. Res.*, in press.
(31) As repeated freeze–thaw cycling does not change the frozen gel spectrum, it seems unlikely that significant variations in the proportions of the two states are induced by the freezing process.
(32) Ablett, S.; Clark, A. H.; Rees, D. A. *Macromolecules* **1982**, *15*, 597–602.
(33) Meiboom, S.; Gill, D. *Rev. Sci. Instrum.* **1958**, *29*, 688–691.
(34) Welsh, E. J.; Bailey, J.; Chandarana, R.; Norris, W. E. *Prog. Food Nutr. Sci.* **1982**, *6*, 45–53.
(35) Hizukuri, S.; Kaneko, T.; Takeda, Y. *Biochim. Biophys. Acta* **1983**, *760*, 188–191.

(36) Gidley, M. J. *Carbohydr. Res.* **1987**, *161*, 301-304.
(37) Rees, D. A. *J. Chem. Soc. B* **1970**, 877-884.
(38) Torsion angles ϕ and Ψ are defined by H(1)-C(1)-O(1)-C(4') and H(4')-C(4')-O(1)-C(1), respectively,[37] and are the major determinants of polymer conformational variations.[20]
(39) Imberty, A.; Chanzy, H.; Perez, S.; Buleon, A.; Tran, V. *Macromolecules* **1987**, *20*, 2634-2636.
(40) Wu, H.-C. H.; Sarko, A. *Carbohydr. Res.* **1978**, *61*, 27-40.
(41) Morris, E. R.; Rees, D. A.; Young, G.; Walkinshaw, M. D.; Darke, A. *J. Mol. Biol.* **1977**, *110*, 1-16.
(42) Stipanovic, A. J.; Stevens, E. S. *ACS Symp. Ser.* **1981**, *No. 150*, 303-315.
(43) Pfannemüller, B. *Int. J. Biol. Macromol.* **1987**, *9*, 105-108.
(44) Pangborn, W.; Langs, D.; Perez, S. *Int. J. Biol. Macromol.* **1985**, *7*, 363-369.
(45) Gidley, M. J.; Bociek, S. M. *J. Am. Chem. Soc.* **1988**, *110*, 3820-3829.
(46) Imberty, A.; Chanzy, H.; Perez, S.; Buleon, A.; Tran, V. *J. Mol. Biol.* **1988**, *201*, 365-378.
(47) Imberty, A.; Perez, S. *Biopolymers* **1988**, *27*, 1205-1221.

Rheology of Solutions of Rodlike Polymers: Theory and Comparison with Experiments

Burak Erman and Ivet Bahar

School of Engineering, Bogazici University, Bebek 80815, Istanbul, Turkey

Patrick Navard*

Centre de Mise en Forme des Materiaux, Ecole Nationale Superieure des Mines de Paris, Sophia Antipolis, 06560 Valbonne, France. *Received October 23, 1987; Revised Manuscript Received April 6, 1988*

ABSTRACT: The Doi theory (*J. Polym. Sci., Polym. Phys. Ed.* **1981**, *19*, 229) of concentrated solutions of rodlike particles is compared with the recent treatment of Bahar and Erman (*J. Polym. Sci., Polym. Phys. Ed.* **1986**, *24*, 1361) of the lattice theory of rods in a potential flow field. The Doi theory is modified by introducing a flow term to its effective mean-field potential, similar to that of the lattice treatment. Results of calculations based on the modified Doi theory are in agreement with existing viscosity concentration data on α-helical poly(benzylglutamate) in *m*-cresol. At relatively low shear rates, the experimentally observed sharp maximum in viscosity is found to be located in the biphasic region. In this region the orientational order parameter and viscosity are double-valued. The characteristic features of the biphasic regime predicted by the theory are discussed. The viscosity–concentration curves exhibit smoother maxima at higher shear rates, although no phase separation is predicted by the theory. As the flow rate is further increased, the maximum gradually disappears in agreement with experiments. Also, the experimentally observed Newtonian plateau in the plots of viscosity against shear rates is obtained by the theory. Quantitative agreement between theory and experiment fails at high shear rates.

Introduction

Equilibrium statistics of solutions of rodlike particles have been formulated by Onsager,[1] Isihara,[2] and Flory.[3] These theories show that a solution of rodlike polymers separates into an isotropic and an anisotropic phase above a critical concentration, v^*_2, depending on the axial ratio of the molecules. The presence of a critical concentration results solely from the effects of steric repulsions between the rodlike solute particles. It was also shown by theory[3] that at a higher concentration v_2^A, the isotropic phase becomes unstable and the solution becomes completely anisotropic. The treatment of the problem according to lattice statistics by Flory has been improved[4] where distribution of orientations of rods are calculated rigorously and the effects of thermotropic interactions[5] are included. The basic predictions of the equilibrium theory lead to the following relations between v^*_2, v_2^A, and the axial ratio, x, of rods

$$v^*_2 = \frac{8}{x}(1 - 2/x) \qquad v_2^A = 11.6/x \tag{1}$$

which are in qualitative agreement with results of various experiments on solutions of α-helical poly(γ-benzyl-L-glutamate) in different solvents.[6-11]

The concentrations v^*_2 and v_2^A may be determined by steady flow viscosity measurements. Results of experiments in this field have critically been discussed by Matheson[12] where it is deduced that the maximum in the viscosity–concentration diagram should lie between v^*_2 and v_2^A.

The equilibrium lattice treatment of Flory[3] has been modified by Marrucci and Ciferri[13] by superposing a flow potential on the Gibbs free energy of the quiescent solution. Their analysis have recently been improved by Bahar and Erman[14] by adopting the more recent lattice treatment[4] of Flory and Ronca. It has thus been possible to extend the statistical theory for quiescent solutions to systems in steady-state potential flows for which the concentration dependence of flow-induced orientations and transitions may be calculated as a function of the imposed flow field.

Dynamics of solutions of rodlike molecules have been studied by Doi[15] and Doi and Edwards.[16] Uncrossability of the rods due to steric repulsions, which is the fundamental feature of the lattice treatment, has been incorporated into the kinetic equations governing the behavior of rods in concentrated solutions. The theory has later been extended by Doi[17] to be valid at all concentrations. In addition to predicting the presence of v^*_2 and v_2^A, the theory of Doi provides with a constitutive equation that relates the components of the stress tensor to the degree of orientation at vanishingly small shear rates. When solved numerically, the Doi equations may provide a description of the rheological behavior of rigid-rod lyotropic polymers. An attempt was recently made by Metzner and Prilutski[18] where predictions of the Doi theory were com-

0024-9297/89/2222-0358$01.50/0